

Carbon and oxygen isotopic variation in Tamil Nadu carbonatites, south India

M. K. Pandit^{*†}, A. N. Sial[‡], G. B. Sukumaran[§], S. Ramanathan[§] and V. P. Ferreira[†]

^{*}Department of Geology, University of Rajasthan, Jaipur 302 004, India

[‡]NEG LABISE, Federal University of Pernambuco, Recife, Brazil

[§]Department of Geology, Presidency College, Chennai 600 005, India

Carbonatites of Tamil Nadu (Samalpatti, Sevattur, Hogenakkal and Pakkanadu–Mulakkadu area), tectonically emplaced along faults/fractures of Neoproterozoic Koratti Fault Zone are predominantly calcio-carbonatite to ferro-carbonatite. Their magmatic origin is indicated by intrusive nature, association with alkaline-peralkaline complexes, degree and extent of fenitization and presence of diagnostic accessory mineral phases. The stable isotopic ratios ($\delta^{13}\text{C}$ and $\delta^{18}\text{O}$) reported in the present work provide conclusive evidence of their magmatic origin. Enrichment of ^{18}O in some of the ferrocarnatites appears to be a post-magmatic phenomenon and can be attributed to low temperature hydrothermal alteration.

CARBONATITES, on account of their rarity in occurrence, unique mineral assemblages, deep-seated origin and association with continental rift zones, have acquired immense significance in understanding the evolution of sub-continental upper mantle. Lower viscosity of carbonate liquids allows them to sample larger volume of mantle and their Nd and Sr abundances (well in excess of crustal values) also buffer the possible effects of crustal overprinting^{1,2}.

In India, carbonatites were first reported from Amba Dongar in Gujarat^{3,4}. Subsequently, a number of carbonatite occurrences became known and five major carbonatite-alkalic complexes have been identified (Figure 1). These are associated with major rifting events during late Proterozoic and Cretaceous–Tertiary periods, in correspondence with global rifting phenomena. Indian carbonatite occurrences have been compiled by Krishnamurthy⁵ and their tectonic corroboration has also been attempted by Srivastava and Hall⁶. Absence of systematic geochemical and isotopic data on Indian carbonatite complexes is notable except Ambadongar carbonatite complex, which so far, remains to be the best studied one¹. The present study focuses on petrogenetic implications of high precision, carbon and oxygen isotopic ratios from four major carbonatite complexes of Tamil Nadu (Sevattur, Samalpatti, Hogenakkal and Pakkanadu–Mulakkadu) forming a part of Craton Charnockite Mobile Belt in south India.

Tamil Nadu carbonatites (type IV carbonatites of

Borodin⁷), first described by Deans and Powell⁸ and subsequently studied by others^{9–11}, occur as fracture fills, dykelets, veins and lensoid bodies within Precambrian ultramafics, alkaline complexes and charnockites. These carbonatites are genetically related to the associated syenites and nepheline syenites and tectonically emplaced along NE-SW trending Koratti Fault Zone¹² (Figure 1).

The Sevattur carbonatites occur as arcuate outcrops (with inward dips) along the periphery of pyroxinite, syenite, fenite (fenitized pyroxinite and syenites) body. Calcite-rich sovite, dolomitic sovite and ankeritic carbonatite of the complex (in order of decreasing age) define temporal and spatial relationship with each other⁵. Sovite, representing an older magmatic phase, is confined to the southern part of the complex whereas relatively younger types occupy the central part. Carbonatite bodies in contact with country rock have fine-grained chilled margins and show gradual increase in grain size towards central part. Coarse-grained sovite weathers into a typical reddish brown appearance.

The Samalpatti carbonatites occur as discontinuous, arcuate dykes and veins intruding the dunite–pyroxinites within a dunite–pyroxinite–syenite complex⁵. The whole complex shows intrusive relationship with the hornblende–epidote bearing basement gneisses. The carbonatites range from sovite to ankeritic and pegmatitic types¹³.

The carbonatites of Mulakkadu–Pakkanadu region occur as small dimension, concordant, fracture fills and

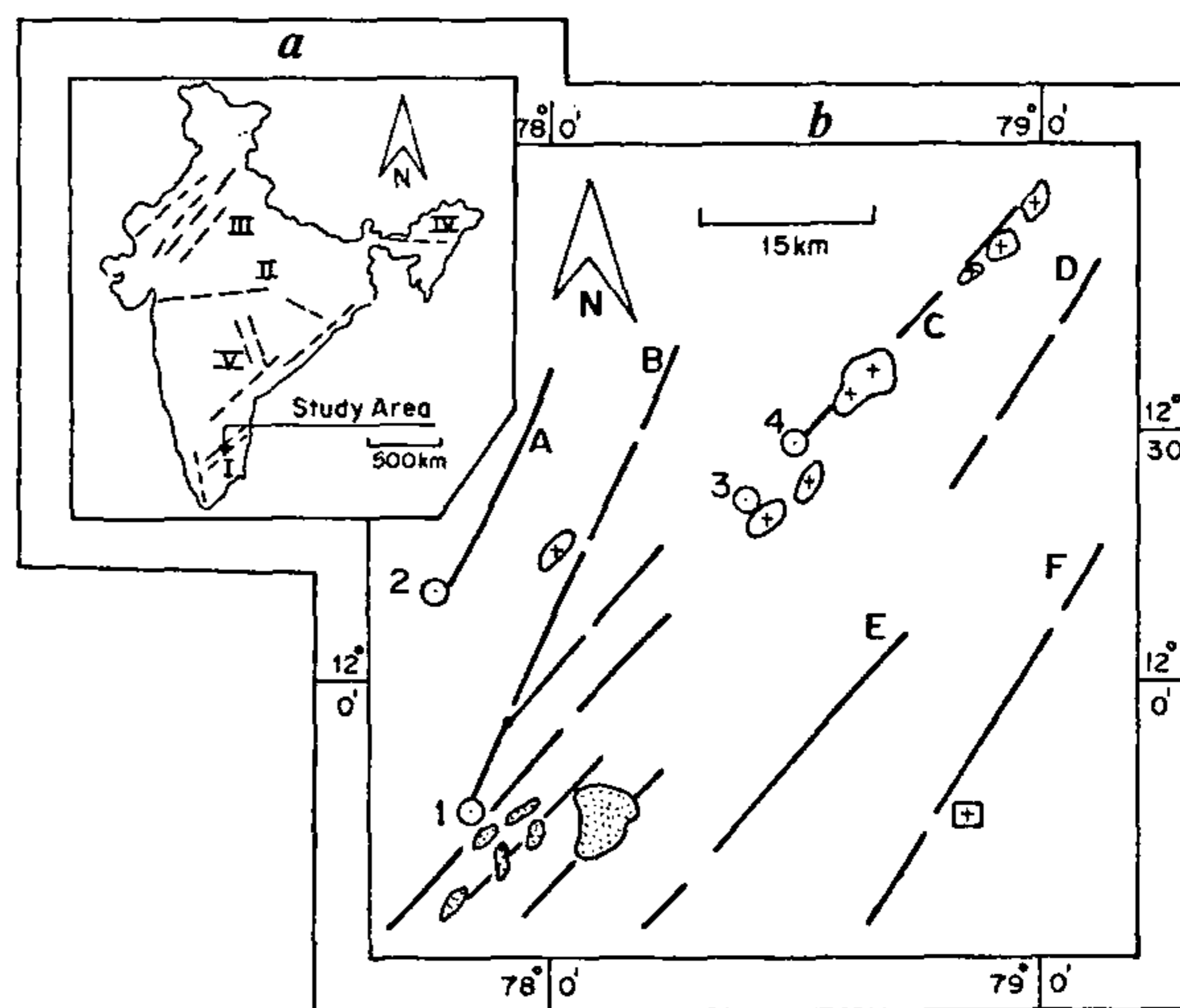


Figure 1. *a*, Map of India showing carbonatite-related tectonic features and location of study area. I, Eastern Ghat Belt; II, Narmada; III, Aravallis; IV, Assam–Meghalaya; V, Cuddapah–Godavari rift zones. *b*, Lithotectonic map of Koratti Fault Zone in Charnockite Mobile Belt showing carbonatite occurrences at Pakkanadu–Mulakkadu (1), Hogenakkal (2), Samalpatti (3) and Sevattur (4) and associated faults (A and B, Mettur faults; C, Main fault; D, Amirdi fault; E, Kottapatti fault and F, Attur fault) and alkalic complexes (stippled area, pyroxinite–dunite and +, syenite). Maps modified after Krishnamurthy⁵.

[†]For correspondence.

dykelets within pyroxinite body and as discordant bodies within syenite, emplaced along a NE-trending fault (subsidiary of Attur Fault). The carbonatites are mainly sovite and ankeritic types. A few occurrences of ijolites, occurring as inclusions within syenite-fenites are present along the margins of pyroxinites and carbonatites¹⁴.

The Hogenakkal carbonatite complex is quite distinct from other carbonatite complexes of Tamil Nadu for being emplaced within Archaean charnockites. The carbonatites form a series of discontinuous bodies within two subparallel NNE-SSW trending pyroxinite dykes, intruding charnockites. The carbonatites range from sovite to calcite-bearing pyroxinites. The sovites are coarse grained and pinkish grey.

The carbonatites demonstrate textural diversity, ranging from coarse grained to fine grained (at places, porphyritic) with rare pegmatoid varieties. Modal mineral heterogeneity (particularly in minor minerals) is another notable feature. Calcite is the most abundant mineral, besides dolomite and less abundant ankerite and siderite (Samalpatti and Pakkanadu). Volumetrically subordinate silicate phases comprise of biotite, riebeckite, diopside and phlogopite. Magnetite and apatite (up to 20% in Hogenakkal area) are the other minerals noticed besides trace abundances of sphene, monazite, allanite, etc.

Mutual relationship of mineral grains indicates early crystallizing silicate phase associated with apatite and magnetite crystallization, followed by main carbonate minerals. In a few cases, the banding in calcite twin planes is controlled by early formed apatite. Corroded grain margins in amphiboles and pyroxenes indicate some degree of disequilibrium between early formed crystals and the melt. Biotite laths with corroded margins (during remelting of congealed magma) are usually surrounded by secondary growth of phlogopite mica. Rounded and ellipsoid apatite grains have smooth outline resulting from attrition during movement of the melt.

The following mineralogical variants have been identified on the basis of modal abundance of various mineral phases: (i) Sovite: mica, apatite-bearing sovite and mica, pyroxene, apatite-bearing sovite; (ii) Dolomitic sovite; (iii) Ankerite to para-ankeritic carbonatite; (iv) Calcitic pyroxinites.

Major element analysis was carried out by conventional wet chemical method and the trace elements were determined at NGRI, Hyderabad, on ICP-MS Plasma Quad, using international standards. Carbon and oxygen isotopes were determined mass spectrometrically on VG Isotech, Stable Isotope Ratio Analyser, at NEG LABISE, Recife. Oxygen and carbon were extracted as CO₂ by reaction with 100% phosphoric acid¹⁵ at 25°C for 24 to 48 h. In case of slow reacting ankeritic carbonatites, a longer reaction period (7 to 10 days) was preferred instead of increasing the reaction temperature to 50°C. BSC (Borborema Skarn Calcite) has been used as the

reference gas for measurements. This was calibrated against NBS-19 and NBS-20 before the run. Running NBS-20 as unknown against BSC, we got the $\delta^{13}\text{C}$ as -1.05 per mil and $\delta^{18}\text{O}$ as -4.10 (PDB) which are very close to the values reported by National Bureau of Standards, USA (-1.06 and -4.4 per mil, respectively).

The major elements are represented as wt% oxides, isotopes as standard per mil notations ($\delta^{18}\text{O}$ relative to SMOW and $\delta^{13}\text{C}$ relative to the PDB standard), the analytical precision for the isotopic ratios has also been mentioned. The major element analysis (including Rb and Sr) is given in Table 1 and the carbon and oxygen isotope ratios in Table 2.

The Tamil Nadu carbonatites are quite variable in terms of major oxides, particularly SiO₂, Fe₂O₃, CaO and MgO. In the CaO-MgO-(FeO+Fe₂O₃+MnO) diagram these plot in the calciocarbonatite (sovite) to ferrocyanatite fields¹⁶ (Figure 2). A significant geochemical feature of calciocarbonatites is the low concentrations of MgO (1.20 to 4.10%), Na₂O (0.14 to 2.00%) and K₂O (0.11 to 1.5%) and their inverse relationship with CaO. An increase in Fe, Mg and Mn from calciocarbonatite to ferrocyanatite (Figure 2) is quite similar to carbonatite trends¹⁷. Distinct covariance between P₂O₅ and CaO is also well demonstrated. The enrichment of Sr over Rb is a diagnostic feature of calciocarbonatites, however, the ferrocyanatites have a preponderance of Ba over Sr.

For a greater degree of confidence, 15 samples were analysed for stable isotopic compositions. The values obtained for each locality are remarkably similar, so only representative analysis from each locality has been included in discussion. However, the range of the isotopic ratios has been mentioned along with the $\delta^{13}\text{C}$ and $\delta^{18}\text{O}$ values (Table 2). The range of $\delta^{13}\text{C}$ and $\delta^{18}\text{O}$ for primary igneous carbonatites, proposed to be between -4 and -8 per mil and +6 and +10 per mil by earlier workers, has been subsequently expanded to -2 to -8 and +6 to +12 per mil (ref. 18). The stable isotopic signatures of the carbonatites indicate homogeneous $\delta^{13}\text{C}$ values (-3.634 to -6.436 per mil) and variable $\delta^{18}\text{O}$ (+7.780 to +24.032 per mil). The distinctive $\delta^{13}\text{C}$ signatures confirm the primary nature and mantle origin for these carbonatites (Table 2). There is a lack of systematic correspondence between $\delta^{13}\text{C}$ and $\delta^{18}\text{O}$ values (Figure 3). Some of the samples plot outside the mantle box, although still well within the range of crystal fractionation¹⁸. The O and C isotopic data allow the discrimination of these carbonatites into two types: (i) Those with $\delta^{18}\text{O}$ and $\delta^{13}\text{C}$ values corresponding with mantle values (mainly calciocarbonatites); (ii) Those with high $\delta^{18}\text{O}$ values, not correlatable with magmatic $\delta^{13}\text{C}$ values (mainly ferrocyanatites).

A large number of databases would always bring more confidence while drawing inferences, however, the two

Table 1. Major element composition of Tamil Nadu carbonatites

S. no.	1	2	3	4	5	6	7
Sample no.	SVT/4	PALL/4	BG/17	OK/27	MK/28	H/46	PK/8
SiO ₂	1.41	25.93	22.90	25.97	1.50	0.20	6.72
TiO ₂	0.01	1.13	1.60	1.30	0.05	0.03	0.55
Al ₂ O ₃	1.49	5.20	3.82	4.60	1.10	0.35	1.88
Fe ₂ O ₃	1.99(t)	9.56	5.12	9.71	2.30	Tr	2.90
FeO		3.00	0.90	2.97	2.50	0.30	6.20
MnO	0.20	2.37	Tr	1.97	0.25	Tr	0.60
MgO	2.95	7.58	4.20	7.12	2.68	1.20	6.33
CaO	50.73	17.99	35.21	18.00	51.25	54.28	35.12
Na ₂ O	0.31	3.45	1.41	3.20	0.17	0.14	0.52
K ₂ O	0.21	3.09	1.92	3.10	0.12	0.11	1.00
P ₂ O ₅	2.50	1.20	1.00	1.10	4.90	1.12	0.90
CO ₂	36.20	18.50	22.00	18.40	32.30	42.57	34.56
Sr (%)	0.75	0.63	0.63	0.14	1.57	1.22	0.55
Ba (%)	0.20	0.89	0.08	0.58	0.43	0.05	1.13

1, Sevattur calciocarbonatite; 2, 3 & 4, Samalpatti ferrocyanatite; 5, Mulakkadu calciocarbonatite; 6, Hogenakkal calciocarbonatite; 7, Pakkanadu ferrocyanatite. (Sr and Ba were analysed by ICP MS as ppm).

Table 2. Stable isotopic composition of Tamil Nadu carbonatites. Carbon and oxygen isotopes are presented as standard per mil notation relative to PDB (Pee Dee Belemnite) and SMOW (Standard Mean Ocean Water), respectively

Sample number	$\delta^{13}\text{C}$		$\delta^{18}\text{O}$	
	$\delta^{13}\text{C}$	Range	$\delta^{18}\text{O}$	Range
SVT/4	-6.436 ± 0.004	-6.439 to -5.866	+13.155 ± 0.006	+7.985 to +13.155
PALLA/4*	-4.372 ± 0.006		+15.425 ± 0.008	
BG/17*	-3.937 ± 0.005		+11.136 ± 0.007	
OK/27	-3.634 ± 0.011	-3.634 to -3.363	+24.032 ± 0.012	+24.032 to +25.447
MK/28	-3.703 ± 0.002	-3.800 to -3.703	+7.780 ± 0.004	+7.261 to +7.780
H/46	-6.153 ± 0.003	-6.226 to -6.027	+8.375 ± 0.007	+8.079 to +8.375
PK/8*	-5.300 ± 0.006		+8.610 ± 0.005	

*Only one sample has been analysed from the locality.

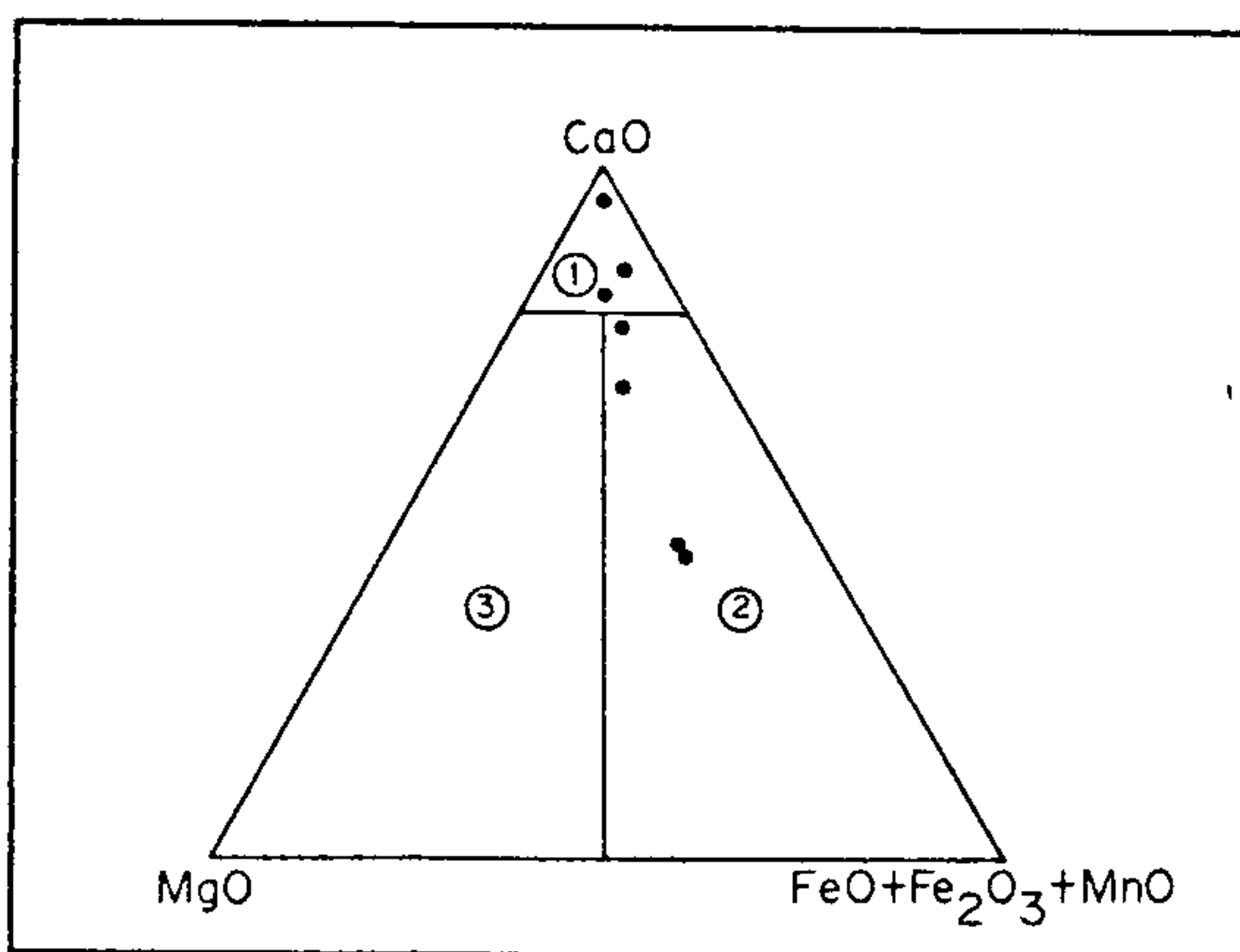


Figure 2. CaO-MgO-Fe₂O₃ + FeO + MnO diagram showing discrimination of carbonatites into calcio-carbonatite and ferro-carbonatite fields¹⁶. 1, Calciocarbonatite; 2, Ferrocyanatite; 3, Magnesiocyanatite.

groups identified in the present work are quite distinct to be mixed up.

The isotopic values in carbonatites vary as a result of differences in the isotopic composition of magma, isotopic fractionation during magma genesis and isotope effects during crystallization¹⁸. Enrichment in the heavier isotopes can also be attributed to Rayleigh fractionation or crustal interaction during emplacement. Enrichment in heavier carbon isotope in a number of carbonatite complexes has been explained by invoking the Rayleigh fractionation model¹⁹⁻²¹. In the present case, the Rayleigh fractionation model cannot be applied due to absence of systematic variation between $\delta^{13}\text{C}$ and $\delta^{18}\text{O}$ values. Further, it cannot explain $\delta^{18}\text{O}$ values greater than +17 per mil (ref. 18). Homogeneity in $\delta^{13}\text{C}$ values also rule out any source heterogeneity to effect isotopic variation. Enrichment in ¹⁸O against magmatic $\delta^{13}\text{C}$ values has been ascribed to post-magmatic processes, particularly low temperature interaction with meteoric waters^{1,21}. The enrichment in ¹⁸O is a common feature of late stage

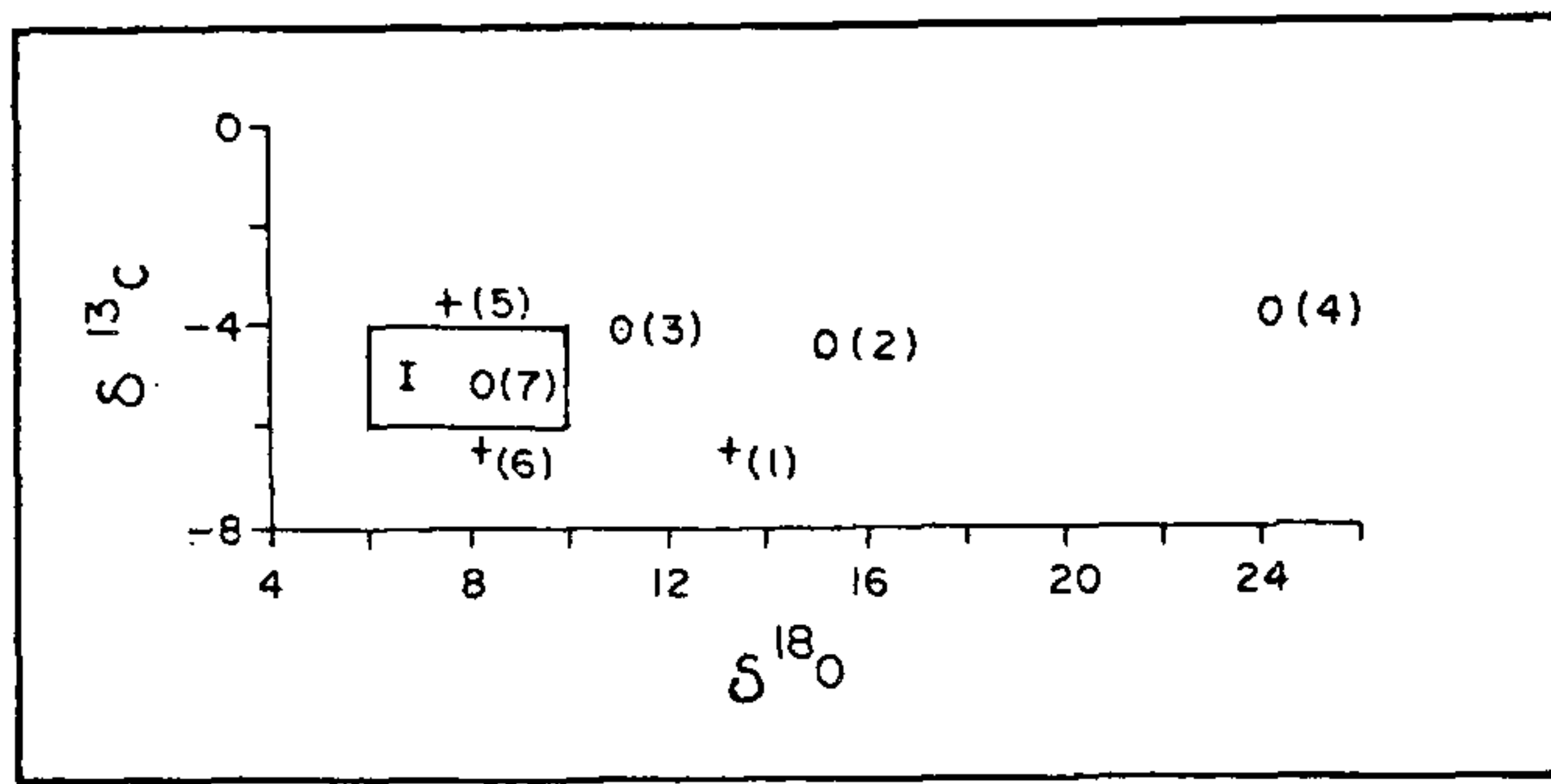


Figure 3. $\delta^{13}\text{C}$ - $\delta^{18}\text{O}$ diagram showing mantle values for $\delta^{13}\text{C}$ and wide range in $\delta^{18}\text{O}$. Mantle carbonatite box¹⁷ (I) is also given for reference. Numbers in parentheses correspond with the serial numbers given in Table 1. Open circle, ferrocarnatite; +, calciocarnatite. Note ^{18}O enrichment in ferrocarnatites.

carbonatites, richer in ankerite and dolomite²². Similar conclusions have been drawn for Amba Dugar carbonatites of western India^{1,23}. In the present case the enrichment in heavier ^{18}O isotopic fraction, thus, is a result of superposed events caused by interaction with hydrothermal fluids. Water is an important component of carbonatites, particularly during late stages of the evolution of magma. Any hydrothermal alteration would result in upward shift in the $\delta^{18}\text{O}$ values (beyond 6 per mil). It is only at a temperature above 270°C that the calcite-water fractionation becomes larger than +6 per mil. Water-rich fluids responsible for high temperature ($>400^\circ\text{C}$) alteration are usually of magmatic origin and would not effect significant shift in O isotopic composition. Shallow level complexes demonstrate more variation in the O isotopic composition. Elevated $\delta^{18}\text{O}$ values (of ferrocarnatites) can be attributed to sub-solidus groundwater interaction. The carbonate-water fractionation and typically negative $\delta^{18}\text{O}$ values for meteoric groundwaters necessitate a low temperature ($>250^\circ\text{C}$) interaction^{18,24}. Extreme enrichment in $\delta^{18}\text{O}$ ($>+20$ per mil) would require a very low temperature ($\leq 50^\circ\text{C}$) during groundwater interaction¹. Lower abundance of carbon (relative to oxygen) in the crust does not permit large scale C isotopic variation which remains unaffected from any low temperature, carbon absent hydrothermal process. As established in the foregoing discussion, and the absence of corresponding variation in $\delta^{13}\text{C}$, the variation in $\delta^{18}\text{O}$ can only be explained by low temperature hydrothermal alteration. The carbon isotopic fractionation between carbonatite melt and CO_2 dissolved in silicate melt would be quite similar.

The stable isotopic data, presented above, indicate almost homogeneous, magmatic $\delta^{13}\text{C}$ values and widely variable $\delta^{18}\text{O}$ values. Significant observations can be summarized to conclude:

- The Tamil Nadu carbonatites have close spatial and temporal relationship with Neoproterozoic rifts and lineaments.

- Textural relationships indicate early crystallization of non-carbonate phases (oxides, silicates, phosphates). Smooth, ellipsoidal surfaces of early formed apatite indicate attrition during emplacement of melt along narrow fault/fracture zones. Melt-crystal relationship is also manifested in development of phlogopite rims around biotite laths and corroded margins of riebeckite.
- These have modal mineralogical heterogeneity, however, geochemically these are calciocarnatite (sovite) and ferrocarnatite (ankerite to para-ankeritic types).
- Homogeneous $\delta^{13}\text{C}$ values, corresponding with mantle values, underline primary nature and mantle source and similar depth of generation. Significant enrichment in heavier ^{18}O isotope in ferrocarnatites without corresponding enrichment in ^{13}C isotope is a result of low temperature alteration by meteoric water interaction. The calciocarnatites are relatively unaffected by such post-emplacement interaction which is more pronounced in ferrocarnatites.
- Close association of carbonatites with the alkaline complexes is a possible manifestation of their common petrogenetic lineage.
- Geochemical signatures and field relations of these carbonatites and associated alkaline complexes indicate a carbonated alkalic magma from which carbonates were derived by liquid immiscibility. The inferences need to be substantiated by detailed trace and rare earth element data and mineral chemistry.

In conclusion, it can be said that the Tamil Nadu carbonatites are truly magmatic in origin and have undergone variable degree of post-magmatic alteration by meteoric waters.

1. Simonetti, A., Bell, K. and Viladkar, S. G., *Chem. Geol.*, 1995, **122**, 185-198.
2. Bell, K. and Blenkinsop, J., *Carbonatites: Genesis and Evolution* (ed. Bell, K.), Unwin Hyman, London, 1989, pp. 278-300.
3. Subramaniam, A. P. and Parimoo, M. L., *Nature*, 1963, **198**, 563-564.
4. Sukhwala, R. N. and Udas, G. R., *Sci. Cult.*, 1963, **2**, 1-10.
5. Krishnamurthy, P., *Expl. Res. Atomic Miner.*, 1988, **1**, 88-115.
6. Srivastava, R. K. and Hall, R. P., in *Magmatism in Relation to Diverse Tectonic Settings*, Oxford and IBH, New Delhi, 1995, pp. 136-154.
7. Borodin, L. S., *Dokl. Sov. Geol. Probl.*, 1960, **16**, 88-99.
8. Deans, T. and Powell, J. L., *Nature*, 1968, **218**, 750-752.
9. Udas, G. R. and Krishnamurthy, P., *Curr. Sci.*, 1970, **37**, 77-78.
10. Borodin, L. S., Gopal, V., Moralev, V. M., Subramanian, V. and Ponikrov, V., *J. Geol. Soc. India*, 1971, **12**, 101-112.
11. Srinivasan, V., *J. Geol. Soc. India*, 1977, **18**, 598-604.
12. Grady, J. C., *J. Geol. Soc. India*, 1971, **12**, 56-62.
13. Subramaniam, V., Viladkar, S. G. and Upendran, R., *J. Geol. Soc. India*, 1978, **19**, 206-216.
14. Sukumaran, G. B. and Ramnathan, S., National Symposium on Precambrian Geology, Madras, 1990 (Abstract).
15. McCrea, J. M., *J. Chem. Phys.*, 1950, **18**, 849-857.
16. Wooley, A. R. and Kemp, D. R. C., in *Carbonatites: Genesis and Evolution* (ed. Bell, K.), Unwin Hyman, London, 1989, pp. 1-13.
17. Keller, J. and Hoefs, J., *IAVCEI Proc. Volcanol.*, 1995, **4**, 113-123.

18. Deines, P., in *Carbonatites: Genesis and Evolution* (ed. Bell, K.), Unwin Hyman, London, 1989, pp. 301–359.
19. Korzhinskiy, A. F. and Mamchur, G. P., *Int. Geol. Rev.*, 1980, **22**, 1390–1396.
20. Reid, D. L. and Cooper, A. F., *Chem. Geol.*, 1992, **94**, 293–305.
21. Simonetti, A. and Bell, K., *J. Petrol.*, 1994, **35**, 1597–1621.
22. Suwa, K., Oana, S., Wada, H. and Osaki, S., *Phys. Chem. Earth*, 1975, **9**, 735–745.
23. Gwalani, L. G., Rock, N. M. S., Chang, W. S., Fernandez, S., Allegre, C. J. and Prinzhofer, A., *Mineral. Petrol.*, 1993, **47**, 219–253.
24. Hoefs, J., in *Stable Isotope Geochemistry*, Springer, Berlin, 1987, p. 241.

ACKNOWLEDGEMENTS. We thank Gilza for sample preparation for isotopic analysis and R. G. Brasilino for helping in petrographic studies. The isotopic analysis was carried out at NEG LABISE during a fellowship to M.K.P. for which he is thankful to TWAS, Italy for travel assistance and to CNPq, Brazil for financial support. Facilities extended by the Director, Rajasthan University Computer Centre are also thankfully acknowledged.

Received 14 July 1997; revised accepted 21 January 1998

Studies on spin-labelled peptide nucleic acid

XiaoXu Li*, ChenGang Huang[†], Yanguang Wang[†], YaoZu Chen^{††}, LiangRen Zhang*, JinFeng Lu*, LiHe Zhang*

*National Laboratory of Natural and Biomimetic Drugs, Beijing Medical University, Beijing 100083, China

[†]Department of Chemistry, Zhejiang University, Hangzhou 310027, China

Spin-labelled peptide nucleic acid T10 (PNAT10) was synthesized by solid-phase method with Boc strategy. The product was characterized by electron spin resonance (ESR) and time of flight MS (TOF MS) analysis, revealing a facile spin labelling of PNA by *in situ* solid-phase synthesis. The spin-labelled PNA product shows same hybridizing ability as that of native one and may be used in studying the cell membrane permeability of PNA by determination of the ESR signals.

HIGHLY stable analogues of DNA or RNA are of considerable interest in medicinal chemistry and molecular biology due to their possible use as therapeutic agents and as molecular biological tools. Peptide nucleic acid (PNA) is a DNA mimic in which the entire backbone has been replaced by a pseudopeptide backbone composed of *N*-(2-aminoethyl)glycine units^{1,2}. PNA can hybridize to the complementary DNA or RNA and exhibits sequence discrimination and thermal stability equal to

or better than that of DNA^{2–5}. PNA also shows biological effects including *in vitro* transcription and translation modulation and much more biological stability towards proteases and nucleases. These characters make PNA the candidate of choice amongst potential gene-regulating drugs^{6–8}. One of the limitations, however, of PNA to be a feasible gene-regulating drug is that PNA cannot enter cell by passive diffusion because of its poor cell membrane permeability⁹, and some attempts have been made to improve cell uptake of PNA¹⁰. The more convenient and versatile method to evaluate cell membrane permeability of PNA is therefore an impetus for studies on its being used as potential gene-regulating drugs.

Conventional nitroxyl spin-label ESR technique has been extensively applied in pharmacology, molecular biology and biophysics^{11–13}. We propose here a stable nitroxyl-free radical as a reporter molecule of PNA to investigate the transmembrane behaviour of PNA, and spin-labelled PNA might also be applied for gene probe investigation. In this study we practised a facile *in situ* solid-phase synthesis of spin-labelled PNA by condensation of 3-carboxyl-2,2,5,5-tetramethyl-3-pyrroline-1-oxyl with the *N*-terminal amino group of PNAT10 fragment in the course of solid-phase synthesis. The assembled structure is shown in Figure 1, the basic character of spin-labelled PNAT10 is presented and a new method for assessment of transmembrane behaviour of PNA is recommended.

Boc-protected thymynyl monomer was prepared according to the reported method¹⁴. The synthesis of spin-labelled PNAT10 was initiated on a Boc-L-Lys(C1Cbz) modified MBHA resin, the PNAT10 strand was elongated based on thymynyl monomer following standard solid-phase peptide synthesis protocols^{14,15}. After the 10th thymynyl monomer condensation and Boc-deprotection cycle terminated, the *in situ* spin labelling of PNAT10 was carried out continuously using 3-carboxyl-2,2,5,5-tetramethyl-3-pyrroline-1-oxyl (ref. 16) as block for solid-phase synthesis. HF cleavage was used to liberate the free product, purification was conducted by C-18 RP-LPLC (0–40% acetonitrile in 0.1% TFA/H₂O). The final product gave the nitroxyl-free radical signals (three peaks, $g = 2.0019$, $a = 15.8$ G,

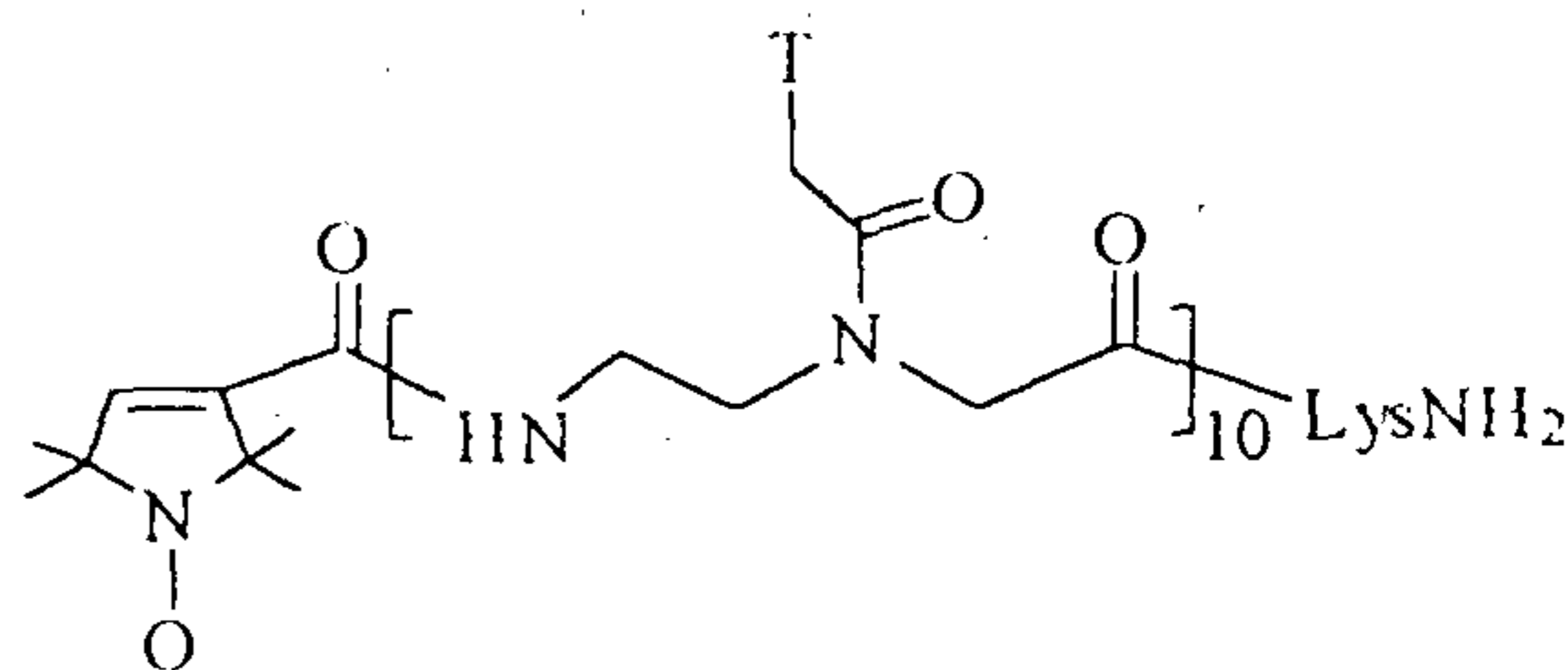


Figure 1. Structure of spin-labelled PNAT10.

[†]For correspondence. (e-mail: mengzhou@bltda.com.bta.net.cn)